Journal of Magnetism and Magnetic Materials 394 (2015) 229–236

Contents lists available at ScienceDirect

Journal of Magnetism and Magnetic Materials

journal homepage: www.elsevier.com/locate/jmmm

Dynamic magnetization models for soft ferromagnetic materials with coarse and fine domain structures

S.E. Zirka [a,*], Y.I. Moroz [a], S. Steentjes [b], K. Hameyer [b], K. Chwastek [c], S. Zurek [d], R.G. Harrison [e]

[a] Department of Physics and Technology, Dnepropetrovsk National University, Gagarin 72, 49050 Dnepropetrovsk, Ukraine
[b] Institute of Electrical Machines, RWTH Aachen University, Schinkelstr. 4, 52056 Aachen, Germany
[c] Faculty of Electrical Engineering, Czestochowa University of Technology, al. AK 17, 42-201 Czestochowa, Poland
[d] Megger Instruments Ltd., Archcliffe Road, Dover, Kent, CT17 9EN, UK
[e] Department of Electronics, Carleton University, Ottawa, Canada K1S 5B6

ARTICLE INFO

Article history:
Received 12 July 2014
Received in revised form
16 April 2015
Accepted 27 June 2015
Available online 2 July 2015

Keywords:
Soft ferromagnetic materials
Magnetic losses
Loss separation

ABSTRACT

We consider dynamic models, both numerical and analytical, that reproduce the magnetization field $H(B)$ and the energy loss in ferromagnetic sheet materials with different domain structures. Conventional non-oriented (NO) and grain-oriented (GO) electrical steels are chosen as typical representatives of fine-domain and coarse-domain materials. The commonly-accepted loss separation procedures in these materials are critically analyzed. The use of a well-known simplified ("classical") expression for the eddy-current loss is identified as the primary source of mistaken evaluations of excess loss in NO steel, in which the loss components can only be evaluated using the Maxwell (penetration) equation. The situation is quite different in GO steel, in which the loss separation is uncertain, but the total dynamic loss is several times higher than that explained by any version (numerical or analytical) of the classical approach. To illustrate the uncertainty of the loss separation in GO steel, we show that the magnetization field, and thus the total loss, in this material can be represented with equal accuracy using either the existing three-component approach or our proposed two-component technique, which makes no distinction between classical eddy-current and excess fields and losses.

1. Introduction

The reliable estimation of energy loss in ferromagnetic sheet materials remains an important and much-discussed problem, both theoretically and practically. It is crucial for designers of electrical machines and transformers, as well as for materials-science engineers engaged in the optimization of morphological properties of electrical steels such as texture and grain size. Although these discussions are largely due to an incomplete understanding of the underlying physics, many are the result of making no distinction between ferromagnetic materials with dissimilar domain structures, i.e., dynamic correlation sizes. Typical examples of such significantly different materials include the conventional non-oriented (NO) and grain-oriented (GO) electrical steels, as considered in this paper.

Because of its small magnetic anisotropy, NO steel, also called dynamo steel, is commonly used in electrical motors and generators, which are applications where the magnetic flux changes direction in the plane of the sheet. Due to its spatially random domain structure and small grain size, NO steel approaches a homogeneous isotropic material, in which the magnetization dynamics can be described, to a good first approximation, by classical Maxwell equations [1–3].

The situation is quite different in anisotropic GO steel, which is the major core material for large transformers, reactors, and other devices in which the flux is predominantly unidirectional. Soon after its invention by Goss [4] in 1934 and its industrialization by ARMCO in the 1940s, it was recognized that the total loss in this material is anomalously higher than could be explained using the classical approach, even when using an accurate hysteresis model to link the magnetic field H and induction B, when solving the appropriate Maxwell's equations. Although the problem of the anomalous (or excess) loss has been the focus of intense research for several decades [5,6], its resolution remains almost unaltered in the sense that no reliable deterministic loss theory has emerged [7,8]. For this reason, a statistical loss model developed in the 1980s [7,9] is widely used as an engineering alternative. The distinguishing feature of this phenomenological (semi-empirical)

* Corresponding author.
E-mail address: zirka@email.dp.ua (S.E. Zirka).

http://dx.doi.org/10.1016/j.jmmm.2015.06.082
0304-8853/

approach is the loss separation principle whereby, irrespective of material domain structure, the total loss W (in J/m^3 per cycle) is decomposed into hysteresis loss W_{hyst}, classical loss W_{clas}, and excess loss W_{exc}

$$W = W_{hyst} + W_{clas} + W_{exc}. \quad (1)$$

Although misconceptions in the loss separation approach have been reported in the literature [8,10,11], and there is no room for W_{clas} in numerous physical models of coarse-domain materials (fairly complete reviews can be found in Refs. [5,12–14] this three-term loss representation has found a wide range of applications due to its simplicity and functionality. Besides, the loss separation is definitely possible in fine-domain materials (NO steels) if, of course, an appropriate numerical tool [2,3,15] is employed. Unfortunately, this is seldom the case, and frequently no distinction is made between GO and NO steels in the engineering literature [16–18]. This has led to an admixture of separate notions relating to different materials. Here we attempt to analyze both these different materials in a single paper.

A first theme of the paper is to point out the dangers concealed in the inappropriate application of loss separation to NO steels. These result from an uncritical use of the well-known approximation for the classical eddy-current loss [5,7,9]

$$W_{clas} = \frac{\sigma(d\pi B_p)^2}{6} f \quad (2)$$

This is derived by assuming a uniform sinusoidal induction, with peak value B_p and frequency f, in a magnetically linear ferromagnetic sheet of thickness d and conductivity σ.

The widespread use of Eq. (2) in the literature has often led to distorted pictures of real processes, and has resulted in numerous "correction" techniques [19–21], often using the ideas of skin-effect and skin depth, which lose their original meanings being applied to magnetically nonlinear media [22].

A separate theme of this paper is to demonstrate that, in the case of GO steels, while retaining the framework of the phenomenological approach, dynamic hysteresis loops, and hence total losses, can be reproduced quite accurately without splitting the dynamic loss into "classical" and "excess" components. This result highlights the uncertainty inherent in the idea of separating out the dynamic loss components [14] and serves to partly reconcile its followers and opponents.

In Section 2, we consider the erroneous but widely held view that dynamic losses in electrical steels of any type, such as GO and NO, can be described by means of diffusion-like equations or their circuit equivalents (Cauer networks). This idea has endured for a long time, starting with Refs. [23,24] and reaching recent works [25–27]. Typical errors encountered in both using and ignoring the diffusion (penetration) equations are considered in Section 3. In Section 4 we briefly discuss the physical validity of the loss separation principle (1), as applied to GO steels, and propose alternative versions of the field- (and loss-) separation, having somewhat different underlying concepts, but the same abilities as the transient models [28] that are based on Eq. (1).

2. Classical loss models

In the case of a thin steel strip (with $d \ll l$ in Fig. 1), the classical approach reduces to the solution of the one-dimensional penetration equation [2,3]

$$\sigma \frac{\partial B}{\partial t} = \frac{\partial^2 H}{\partial x^2} \quad (3)$$

This links the magnetic field $H_z(x, t)$ to the magnetic induction

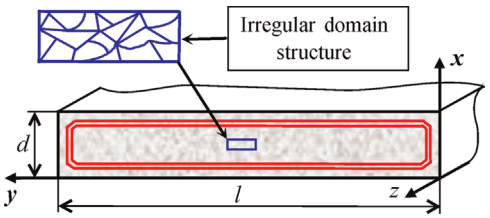

Fig. 1. Classical eddy currents in conventional NO steel with an irregular domain structure.

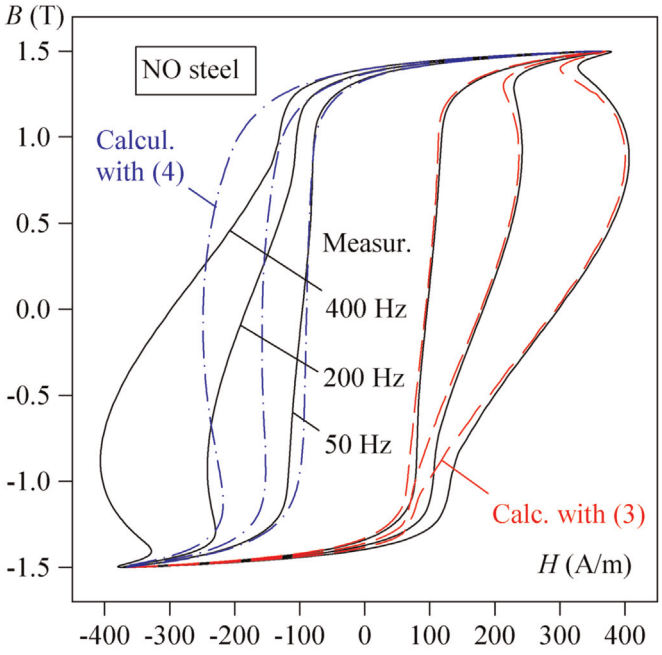

Fig. 2. Dynamic loops of 0.5-mm thick NO steel calculated from Eqs. (3) and (4) versus the measured loops.

$B_z(x, t)$, both directed along the z-axis of a strip with conductivity σ, the x-axis being normal to the strip surface. In posing this problem, all eddy currents are considered y-directed, that is, edge effects are neglected. Only two of their innumerable contours are shown in Fig. 1.

The applicability of Eq. (3) to NO electrical steels is illustrated in Fig. 2. Here the solid curves are dynamic hysteresis loops of 0.5 mm thick steel strips, as measured in an Epstein frame under tightly-controlled sinusoidal induction [29]. The dashed curves on the right-hand side of Fig. 2 indicate the ascending branches of dynamic loops obtained by means of a finite-difference solver (FDS) of Eq. (3), which integrates system (8) in Ref. [3], where the nodal functions $H_i(t)$ and $B_i(t)$, representing the field and induction at the ith "layer" of the sheet, are linked by a static hysteresis model [30].

As seen in Fig. 2, Eq. (3) provides a fairly reliable basis for computing the dynamic loop shapes, and hence their areas, which give the specific energy losses in J/m^3 per cycle. At the same time, a close examination of Fig. 2 reveals small discrepancies between the predicted and measured ascending branches, particularly their lower and upper parts. The larger area of the measured loops, as compared to the calculated loops, indicates the presence of excess loss. It is commonly accepted that this anomalous loss is caused by the domain structure of the ferromagnetic material, which is both fine and highly irregular in the case of NO steel, as depicted in the inset of Fig. 1. The origin of excess loss, when considered to be an addition to the classical loss, is usually thought to be due to microscopic eddy currents associated with the movement of the

domain walls and by additional heat produced by these currents.

The above-mentioned discrepancies between the measured loops in Fig. 2 and the ascending loop branches calculated with Eq. (3) can be eliminated almost completely by introducing a time delay of $B_i(t)$ with respect to $H_i(t)$ in all the "layers" of the sheet. When modeling NO steels, this has been effectively achieved by using a dynamic Preisach model instead of a static one [2], or by introducing magnetic viscosity (the above-mentioned time delay) in addition to the static hysteresis model [3]. As shown in Ref. [3], dynamic loops predicted by the "viscous" FDS, as obtained by integrating system (15) of that reference, practically coincide with the measured loops for both sinusoidal and non-sinusoidal flux densities.

As might be expected, quite distorted loops, as seen in the descending branches of Fig. 2, are predicted at higher frequencies when one uses the well-known low-frequency solution of Eq. (3), which is derived for an abstract homogeneous (non-domain) ferromagnetic material [9],

$$H(t) = H_{\text{hyst}}(B(t)) + K_{\text{clas}}\frac{dB}{dt} \tag{4}$$

Here the field $H_{\text{hyst}}(B)$ is calculated using a static hysteresis model, and the constant $K_{\text{clas}} = \sigma d^2/12$.

These distortions are overlooked if only the total losses are examined. This underlines the fact that a physically sound model must reproduce the shape of dynamic hysteresis loops, not only their areas. Associated mistaken conclusions will be considered in Section 3.

Unlike the case with NO steel, the situation is quite different when the same FDS is applied to GO steel. As shown in Fig. 3, loop 2, obtained by solving Eq. (3) in the absence of the magnetic viscosity, has an obviously different shape and a markedly smaller area (specific total loss) than loop 1, as measured using a computerized setup [29]. Thus, the shortfall in the loss calculated classically, implying the existence of excess loss, is not a consequence of inappropriate mathematics (inaccurate solving of Eq. (3)), but has a physical cause.

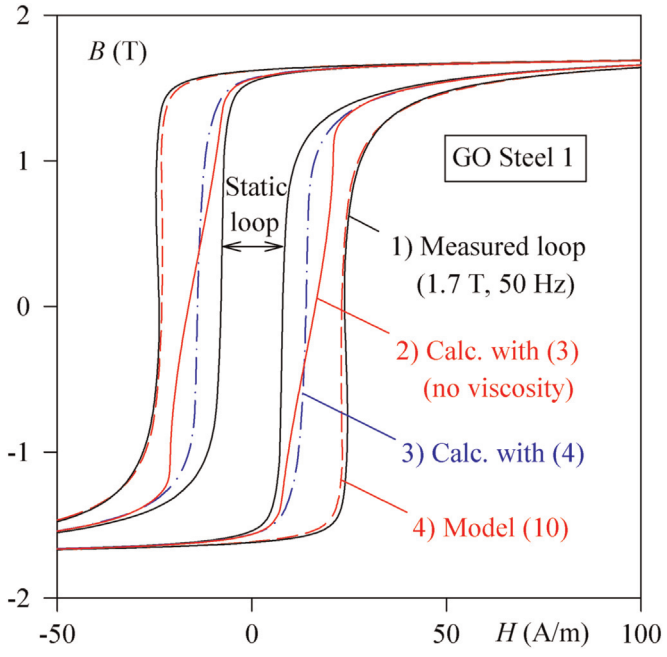

Fig. 3. Dynamic loops of GO Steel 1 calculated using Eqs. (3), (4), and (10) and compared with a measured loop.

3. Typical errors in evaluating excess loss in magnetic materials with fine domain structure

To analyze the errors arising from simplifying assumptions about excess loss, we can rely on the results obtained with finite-difference solver [3] or finite-element solvers [2,15] of Eq. (3). The successful application of the FDS to different NO steels [3,31] operating in a wide frequency range under arbitrary excitations (sinusoidal or non-sinusoidal) confirms its physical validity and allows us to consider the FDS as a reliable tool for evaluating both total loss and its individual components.

The first and probably the main reason of inaccuracies in the loss separation is the use of the "linear" Eq. (2) for the classical eddy-current loss. The error introduced by using Eq. (2) is later included into the third component of total loss [32]. It was reported many times that Eq. (2), being applied at high flux densities, gives underestimated classical loss and therefore overestimated excess loss [1,2,22]. Despite this fact it remains quite typical [21,32,33] to multiply Eq. (2) by the skin-effect function [33], which being less than unity, increases these mistakes.

To evaluate classical eddy-current loss more accurately and explain (at least partly) excess loss, the nonlinear skin effect was analyzed analytically in Refs. [34–36]. To explain the idea developed in the just-mentioned papers, we note that a square-loop approximation of major and minor hysteresis loops in electric steels is more accurate than any linear representation [22,34]. This suggests the use of the saturation-wave-model (SWM) of Wolman and Kaden [37] instead of the conventional linear model leading to Eq. (2). The SWM describes the layer-by-layer flux reversal (from $-B_p$ to $+B_p$ and back) in a ferromagnetic material with a steplike magnetization curve with maximum value $B_{\max}$. It should be noted that analysis of the SWM in the literature is usually restricted to the case where $B_p = B_{\max}$ [9,34]. In general, when $B_p \le B_{\max}$, the well-known expression for the eddy-current loss predicted by the SWM at sinusoidal induction with amplitude B_p can be generalized

$$W_{\text{SWM}} = \frac{\sigma(d\pi B_p)^2}{4} f \frac{B_p}{B_{\max}} \tag{5}$$

Comparing Eq. (5) with Eq. (2) shows that at high flux densities, i.e. at $B_p \approx B_{\max}$, W_{SWM} exceeds W_{clas}. This was the reason to say in Ref. [36], with reference to Ref. [35], that "There is evidence to relate the origin of excess losses to nonlinear properties of magnetic conducting media." This idea permeates a number of papers [27,34–36] and it is not, strictly speaking, completely correct. In fact the "nonlinear skin effect" considered in these papers, does not explain the actual (physical) reason of excess loss, but simply points out the inaccuracy (in some cases) of the linear formula (2). Besides, although the SWM and its modifications [34,35] can indeed explain (partly and qualitatively) the errors of Eq. (2), the practical use of these analytical models is limited by the non-rectangularity of real hysteresis loops and uncertainties of their approximations. In contrast to the root model [37], the analytical models in Refs. [34,35] do not cover the minor and moderate flux densities at which excess loss is also discovered when solving Eq. (3).

It is important to note the significance of Eq. (5) also at low induction where some authors even report negative excess loss values [19,38,39]. These are obtained by the widespread use of the subtraction formula derived from Eq. (1): $W_{\text{exc}} = W - (W_{\text{hyst}} + W_{\text{clas}})$, where W_{clas} is found from Eq. (2). At the same time, the eddy-current losses calculated with Eq. (5) at $B_p < (2B_{\max}/3)$ are less than those found with Eq. (2), and corresponding excess losses are, of course, positive.

At this point we can recall about common explanations of non-physical results obtained with Eq. (2) by means of "eddy-current

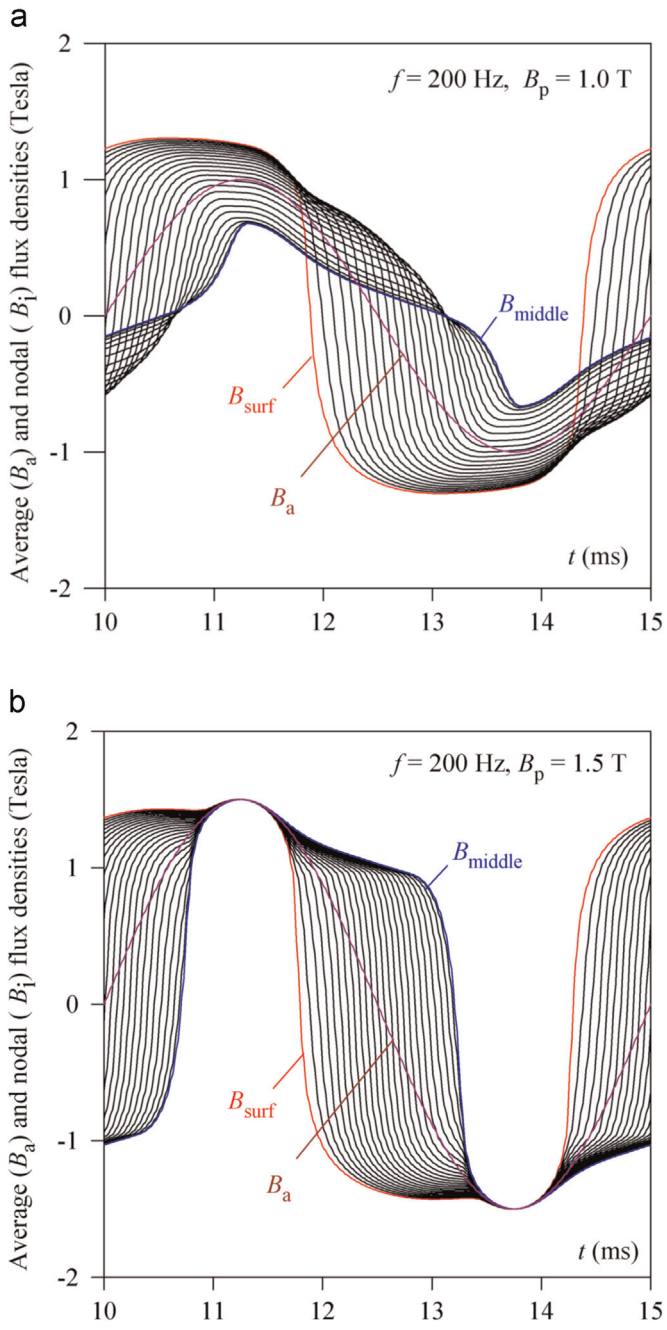

Fig. 4. (a) The presence of skin effect in the NO steel under consideration at moderate induction and (b) its absence at high induction.

shielding" and "skin-effect phenomena" [19,38]. Especially popular is the skin-effect depth, which is often mistakenly applied to ferromagnetic laminations. In this regard, we briefly dwell here on the nonlinear skin effect. The waveshapes in Fig. 4 are nodal (layer) flux densities (at locations from the surface to the middle of the sheet) calculated with Eq. (3) for NO steel at $f=200$ Hz and for moderate ($B_p=1.0$ T) and high ($B_p=1.5$ T) peak values of the average flux density B_a. While an obvious skin effect is seen in Fig. 4(a), calculated for $B_p=1.0$ T, there is in fact no difference between the induction peaks at different sheet depths for $B_p=1.5$ T, which is the working induction for the majority of electric machines.

Fig. 4(b) also shows that numerical solutions of Eq. (3) embrace the behavior inherent in the SWM, including "almost rectangular spatial profiles of magnetic flux density" [36].

Regarding the commonly used formula (2), it is widely used in engineering loss models where its inaccuracies are compensated by fitting "excess loss" terms. However, Eqs. (2) and (4) become excessively approximate when making certain physical assumptions regarding NO steels.

Consider, for example, a "geometrical approach" [40] that ascribes excess loss to certain portions of the dynamic hysteresis loop. In Fig. 5(a) we compare the loop calculated using Eq. (3) with the measured 200 Hz loop shown in Fig. 2. This case roughly corresponds to the 0.65 mm thick NO steel studied at $f=150$ Hz [40]. Similarly to the calculation represented in Fig. 7 of Ref. [40], the loop calculated with Eq. (3) crosses the lower part of the measured loop. This means that the hatched area in Fig. 5 (a) should correspond, according to Ref. [40], to negative excess loss.

To explain the fallacy of this approach, we recall that the dynamic hysteresis loop is the curve $B_a(H_{surf})$ where B_a is the average induction over the sheet cross section, and H_{surf} is the field at the surface of the sheet. So the B-value of any point of the resulting dynamic loop, for example point 0 with $B=0$ in Fig. 5(a), is obtained by averaging the flux densities B_i in all the layers of the sheet, calculated at the same instant t. These values, together with point 0, are the dots in Fig. 5(b), which shows that at $B_a(t)=0$, the layer flux densities lie in the range -0.958 T to $+1.366$ T.

It is, of course, unnatural to think that excess losses are concentrated at some layer of the sheet or at its surface. So there is no point to ascribe excess loss, distributed over the sheet thickness, to some parts of dynamic hysteresis loop [40].

In concluding this section, we should note the inability of the SWM to explain the anomalously high excess loss in GO steel. With this purpose, we can use the anomaly factor η [38,41,42], which is, in the case of the SWM, the ratio of losses calculated with Eqs. (5) and (2): $\eta = W_{SWM}/W_{clas}$. As can be seen from these formulae, the maximum possible value of η in the SWM framework is only 1.5, corresponding to an ideal rectangular hysteresis loop and $B_p=B_{max}$. This cannot explain the much larger values of η observed experimentally in GO steels. For example, the η value for loop 3 in Fig. 3 is 3.3, which is close to the average η for the five GO steels studied in Ref. [42]. This demonstrates that GO steels considered in the next section are in sharp contrast to NO steel with respect to the excess loss value, if we continue to use that term.

4. Domain loss models

Any uncertainties about the existence of excess loss in electrical steels [20,27] disappear when the "classical tools" (3) or (4) are applied to GO steel. This can be seen in Figs. 3 and 6 which show that dynamic loops constructed with these equations have substantially smaller areas than measured loop 1. The GO steel represented in Fig. 3 (it is similar to steel M4 and steel 27Z130 [43]) and the high-permeability grain-oriented (HGO) steel in Fig. 6 will be referred to as Steel 1 ($d=0.255$ mm, $\rho=0.466$ μΩ m) and Steel 2 ($d=0.18$ mm, $\rho=0.47$ μΩ m) respectively.

It is remarkable in Fig. 6 that loop 2, despite its smaller area, exceeds the bounds of the experimental loop 1. Attempts to enlarge the area of loop 2, by introducing a "viscous delay" between nodal $B_i(t)$ and $H_i(t)$, when solving Eq. (3) result in the loops protruding even further from the experimental loop. This shows that, in contrast to NO steels, Eq. (3) is much less appropriate, if appropriate at all, for describing GO steels in which only 20% of the total loss can be typically explained by classical eddy-currents, and the rest is divided roughly equally between hysteretic and excess losses [42,44].

This is the reason why the classical approach to studying GO steels was abandoned in the 1950s–1970s. After the milestone

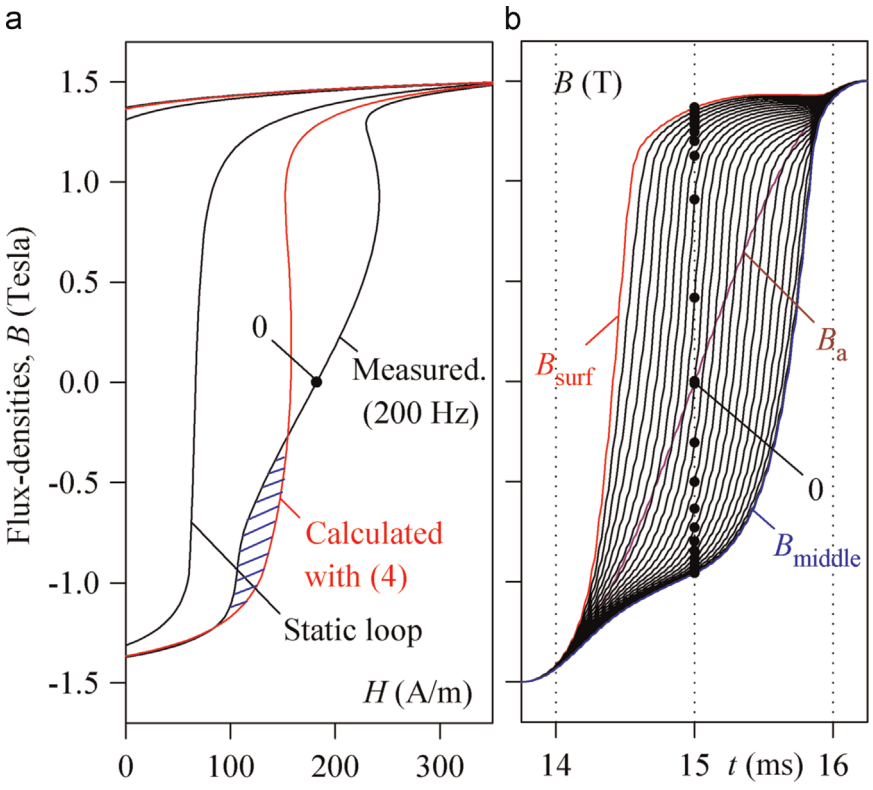

Fig. 5. (a) Dynamic loops and (b) induction waveforms in the NO steel under consideration.

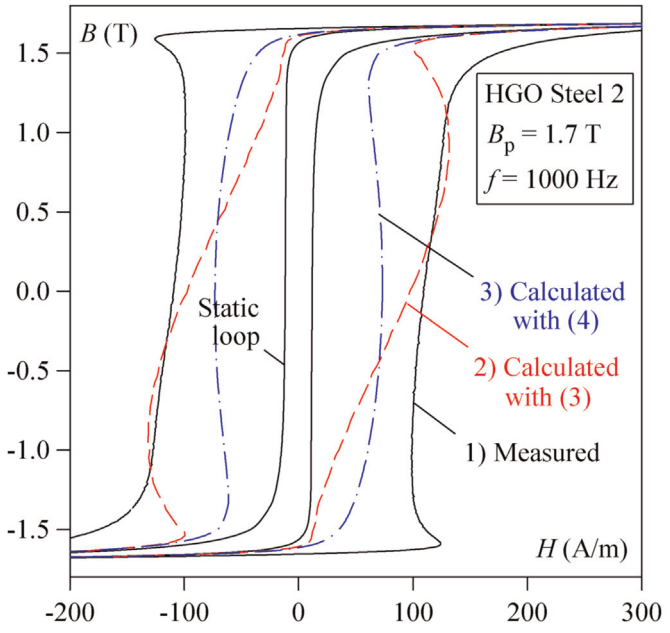

Fig. 6. Dynamic loops of HGO Steel 2 calculated with Eqs. (3) and (4) versus the measured loop.

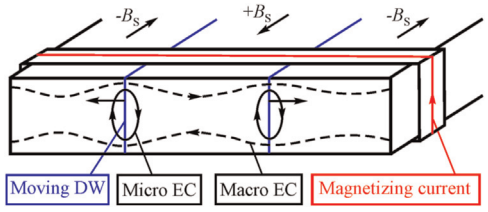

Fig. 7. Microscopic eddy currents induced by moving DWs in the Pry and Bean model [41].

work of Williams, Shockley, and Kittel [45] and the encouraging modeling of Pry and Bean [41], it was anticipated that a unified physical theory accounting for the domain structure of a ferromagnetic material would soon be created. Although such a complete theory still does not exist, its potential features and even its conjectured conclusions occur widely in the literature.

The key loss mechanism of numerous models developed following Pry and Bean [41] is microscopic eddy currents induced by moving domains walls (DWs). Starting with the planar and continuously-moving DWs in Fig. 7, numerous models with bowing, partly pinned and varying numbers of DWs have been proposed.

It is not the purpose of this paper to review the large literature on this subject or to add yet another explanation of magnetization dynamics in materials displaying pronounced domain structures. We only support the idea [14,46] that quasi-static (hysteretic) and dynamic components of a composite magnetization model can be reproduced separately even if their origins have something in common. It should be obvious that DWs undergoing Barkhausen jumps and eddy currents diffusing throughout the whole domain (or several domains) are different entities and should be assessed separately. For example, the quasi-static loops in Figs. 3 and 6 were measured at 0.0033 and 0.004 Hz respectively and there were no signs of a vanishing loop area in the limit of zero frequency.

A successful example of the loss separation idea [5] is the phenomenological (statistical) model (1) justified physically by Bertotti [7,9]. The basic idea of the model is to compensate the experimentally observed loss shortage by providing one more dynamic loss term, namely W_{exc}, as introduced in Eq. (1). When developing the model [7,9], attention was focused on the *loss* prediction, while the shape of dynamic hysteresis loops remained beyond the scope of the study. So, if one prefers to work in the time domain and adhere to the approach in Ref. [9], Eq. (4) can be

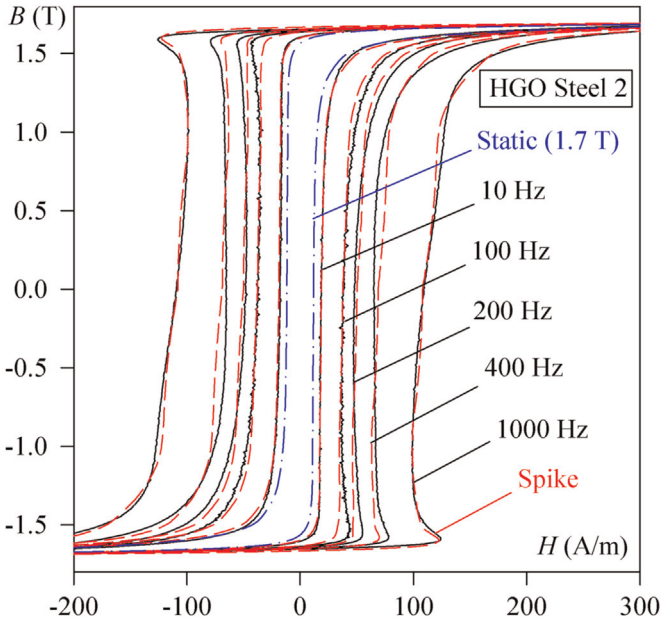

Fig. 8. Dynamic loops calculated from Eq. (9) for Steel 2.

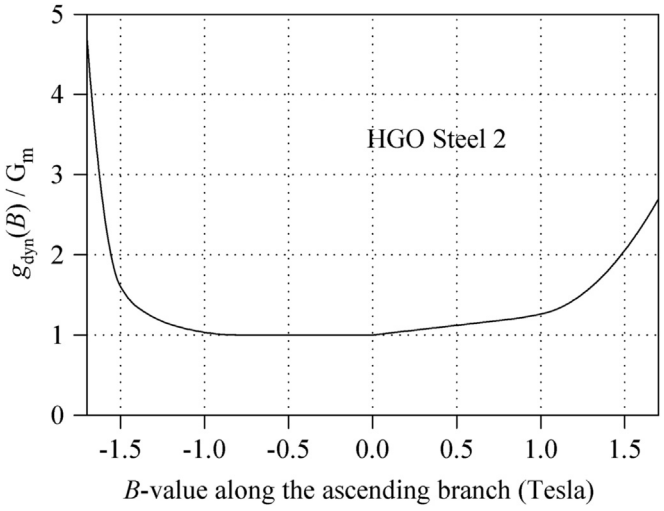

Fig. 9. Normalized function g_{dyn} constructed for HGO Steel 2.

extended to read.

$$H(t) = H_{hyst}(B) + K_{clas}\frac{dB}{dt} + K_{exc}\,\delta\left|\frac{dB}{dt}\right|^{0.5} \tag{6}$$

where δ is a directional parameter (± 1), and coefficient K_{exc} is fitted separately for each B_p. In Ref. [7], this permitted the reproduction of loss-versus-frequency curves $W(f)$ for several different steels measured up to 100 Hz.

A refinement of Eq. (6), proposed in Refs. [28,31], is to use appropriate functions $g_{exc}(B)$ and $\alpha_{exc}(B_p)$ instead of the constant K_{exc} and exponent 0.5 respectively

$$H(t) = H_{hyst}(B) + K_{clas}\frac{dB}{dt} + g_{exc}(B)\,\delta\left|\frac{dB}{dt}\right|^{\alpha_{exc}(B_p)} \tag{7}$$

From a physical viewpoint, the variable $\alpha_{exc}(B_p)$ in Eq. (7) can be explained using the concept of random spatial variations in domain size and thus in domain wall number [47]. Technically, this has allowed us to eliminate the imperfection of Eq. (6), seen in

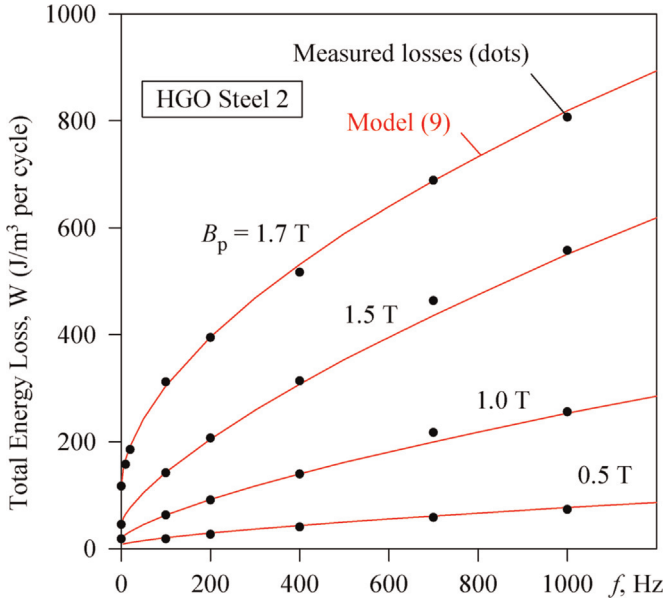

Fig. 10. Loss dependencies calculated from the loop areas.

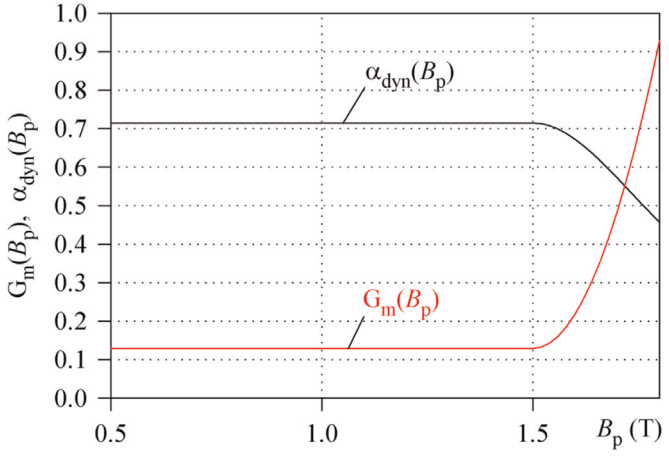

Fig. 11. Acceptable peak-induction dependencies $G_m(B_p)$ and $\alpha_{dyn}(B_p)$ for GO Steel 2.

Fig. 12(a) of Ref. [7], and in Fig. 12 of Ref. [28], where model (6) fitted to the loss values measured at, say, $B_p = 1.5$ T always yielded underestimated losses at $B_p = 1.7$ T. The use of $g_{exc}(B)$ and $\alpha_{exc}(B_p)$ in Eq. (7) can provide quite accurate reproduction of the calculated loops up to 200 Hz and a good coincidence of the measured and predicted total losses up to 400 Hz [28].

At this point a question may arise about the presence of the classical field term in Eq. (7) and, more generally, about the classical loss term in Eq. (1). Even if the microscopic eddy currents, (solid lines in Fig. 7) transform under certain conditions into macroscopic eddy currents (dashed lines), there is no valid reason to account for these by using the "linear" formulae (2) and (4). Some other doubts about the presence of W_{clas} in Eq. (1), but in the case of NO steels, are expressed in Ref. [11].

This returns us to the idea [6] of separating the total loss into only two components, namely hysteresis (DC) and dynamic. In accordance with the inaugural Eq. (1) in Ref. [7], such a loss separation is written as

$$W = W_{hyst} + W_{dyn} \tag{8}$$

Continuing to use functions $g(B)$ and $\alpha(B_p)$, expression (8) leads

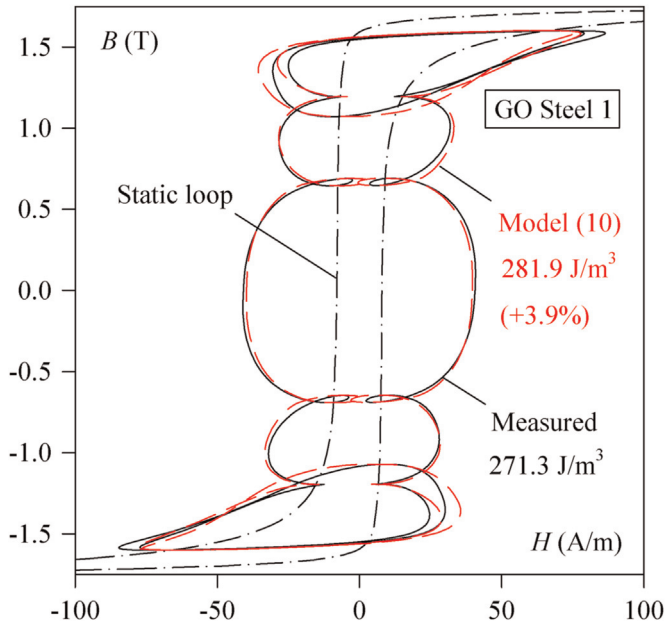

Fig. 12. Dynamic trajectory for GO Steel 1 calculated from Eq. (10) compared with measured data.

to the field separation

$$H(t) = H_{\text{hyst}}(B) + g_{\text{dyn}}(B)\,\delta \left|\frac{dB}{dt}\right|^{\alpha_{\text{dyn}}(B_p)} \tag{9}$$

where $g_{\text{dyn}}(B)$ and $\alpha_{\text{dyn}}(B_p)$ differ from $g_{\text{exc}}(B)$ and $\alpha_{\text{exc}}(B_p)$ in Eq. (7).

Functions $g_{\text{dyn}}(B)$ and $\alpha_{\text{dyn}}(B_p)$ can be found as in Ref. [28]. Selecting a measured dynamic loop, such as loop 1 in Fig. 6, and initially setting $\alpha_{\text{dyn}}(B_p)$ to be constant (typically 0.5–0.8), function $g_{\text{dyn}}(B)$ is constructed so as to obtain a loop calculated with Eq. (9) sufficiently close to the measured loop. In principle, any individual measured loop can be reproduced with Eq. (9) exactly. It can be seen from Eq. (9), that $g_{\text{dyn}}(B)$ represents the variable horizontal gap between dynamic (measured) and static loops divided by $(dB/dt)^{\alpha}$. In practice, function $g_{\text{dyn}}(B)$ can be found by a trial-and-error method, and represented by a computational chain or graph.

The main properties of the functions $g_{\text{exc}}(B)$ in Eq. (7) and $g_{\text{dyn}}(B)$ in Eq. (9) are their minima (G_m) at $B=0$ and their increase with $|B(t)|$. For example, it was found acceptable, in Ref. [44], to represent $g_{\text{exc}}(B)$ for Steel 1 by the expression $G_m(1+kB^2)$, with $G_m=0.38$, and $k=0.576$ (evident dimensions of these values are omitted in this paper).

The calculated loops for Steel 2 (see Fig. 8) were obtained with $\alpha=0.571$ and using the graph in Fig. 9, which shows the function $g_{\text{dyn}}(B)$ normalized to its minimum value, $G_m=0.48$. (The computational chain for $g_{\text{dyn}}(B)$ has a little significance and is not shown in the paper because of its complexity.)

As can be seen in Figs. 6 and 8, dynamic loops observed at higher frequencies are characterized by pronounced "spikes" in their upper and lower parts, which are different for different materials. For example, these "spikes" are enormously large in the metallic glass ribbon modeled in [48]. This makes the modeling an order of magnitude more difficult than for static loops, and shows the uniqueness of each material under both static and dynamic conditions (i.e. in the functions $g_{\text{exc}}(B)$ and $g_{\text{dyn}}(B)$). We re-emphasize, in this regard, that we do not restrict our modeling to loss prediction. Our broader aim is to construct a model that reproduces the *shape* of dynamic hysteresis loops over a wide range of excitations. The loss curves in Fig. 10 are calculated as usual, by evaluating the areas of corresponding dynamic loops.

To reproduce dynamic loops, and thus losses, for any B_p, the minimum (G_m) of the function $g_{\text{dyn}}(B)$ and the exponent α_{dyn} in Eq. (9) should be B_p-dependent. The variable exponent $\alpha_{\text{dyn}}(B_p)$ in Eq. (9) is employed to reproduce the somewhat different curvatures of the loss dependencies $W(f)$ in Fig. 10 at moderate and high B_p. Dependencies $G_m(B_p)$ and $\alpha_{\text{dyn}}(B_p)$ found acceptable for Steel 2 are shown in Fig. 11.

Since Eq. (9) is a time-stepping model which does not "know" the induction waveform and B_p in advance, the dependencies shown in Fig. 11 cannot be used directly. So the value of B_p and thus α_{dyn} and G_m are found dynamically, for example during a transient leading to a steady-state loop. At any reversal of $B(t)$, the interval ΔB between the current and previous turning points is determined. The value of B_p can then be set equal to $\Delta B/2$, allowing one to calculate $\alpha_{\text{dyn}}(B_p)$ and $G_m(B_p)$. These values are retained until the next field reversal.

The same close agreement between predictions of the two-component model (9) and experiment was obtained for Steel 1. It should, however, be pointed out that often there is no need for a "perfect" model, that is, a model that would be equally precise at all flux-densities and at frequencies unusual for given steel. It is, therefore, reasonable to fit the model to the rated induction level and below the highest probable fundamental frequency. This allows one to simplify $g_{\text{dyn}}(B)$ in Eq. (9) and use a constant α. Such a simplified version of Eq. (9) for Steel 1 is

$$H(t) = H_{\text{hyst}}(B) + \delta \left|\frac{0.072}{1-(B/2)^2}\frac{dB}{dt}\right|^{0.74} \tag{10}$$

By using Eq. (10), all the dynamic loops of Steel 1, as obtained in Ref. [28] using the three-component model (7), can be reproduced with the same accuracy. The use of Eq. (10) is illustrated by the dashed line 4 in Fig. 3 and by the calculated trajectory in Fig. 12, which shows the closeness of measured and modeled loops obtained by summation of the 50-Hz, 1.6 T peak fundamental and its 3rd, 7th, and 11th harmonics.

Expression (10) also demonstrates that different forms of the two-component model (9) can be used. The successful application of this model is also in accordance with the general trend in modeling thin ferromagnetic materials without resorting to classical loss contribution [49].

5. Concluding remarks

In this paper, we have tried to outline the situation with loss separation in soft ferromagnetic materials, which is a subject of continuing debate among physicists and engineers. Due to difficulties in their precise classification, we have chosen conventional non-oriented and grain-oriented steels as very different materials in the sense of their domain structures and their different domain sizes with respect to the thickness of the sheet.

We have emphasized that the penetration (diffusion) Maxwell equation in combination with a rate-dependent or rate-independent hysteresis model is only applicable to materials with fine domains (NO steels), and at the same time, it is the only reliable tool for the loss separation. This is explained by the fact that classical eddy currents are the prevailing loss factor in NO steels, whereas the remaining (excess) loss is relatively small. This can lead to the situation in which even a relatively small error in the evaluation of classical loss can result in a large error in the excess loss value. Because of the small contribution of excess loss, this error is not very influential in engineering loss prediction techniques, which are mainly based on the known low-frequency formula (2) for classical eddy-current loss. This is because the inaccurate subdivision of the dynamic loss between classical and

excess components can be effectively corrected by numerous empirical methods.

Quite different situation takes place when the "linear" formula (2) is used in the physical (material) studies based on the excess loss values found by the subtraction technique ensuing from Eq. (1). In particular, the uncritical use of this technique has eventually led to the meaningless ascribing of the "excess loss" to some segments of dynamic hysteresis loop and is fraught with serious errors in evaluating morphological properties of electrical steels.

Another extreme is to declare excess loss absent or even negative. This claim also roots in using Eq. (2) which is sometimes understood literally, i.e. considered as sufficiently accurate formula for evaluating eddy-current loss. We note the drawbacks of analytical studies of this question (the simplifying assumptions make them unreliable), and inaccurate experimental procedures, which are employed to verify numerical solutions of the penetration equation.

Also, it is often not realized that the classical approach, and hence the excess loss concept, lose their validity when studying GO steels that have coarse domains. For reasons explained in Ref. [50], the same is true for thin laminations of NO steel [31] and probably also for many materials in the form of thin sheets or ribbons [48]. In this situation, three-component loss and transient models can be used as palliative solutions. The inherited presence of classical loss (and field) in these models appears to be of inertial origin, so we have tried to omit it as an explicit term and to represent both eddy-current components by a single dynamic term. Successful application of this idea to GO steels suggests that the classical and excess loss (field) terms in the three-component models, which are generally acceptable in engineering practice, can be simply specified as dynamic terms #1 and # 2. This is explained by the fact that in materials in which domain wall spacing is comparable to the sheet thickness, the macroscopic and microscopic eddy currents are hardly to be distinguished.

Acknowledgments

R. Harrison thanks the Natural Sciences and Engineering Research Council of Canada for support under Discovery Grant 1340-2005 RGPIN. The work of S. Steentjes supported by the Deutsche Forschungsgemeinschaft (DFG) and carried out in the research project "Improved modeling and characterization of ferromagnetic materials and their losses".

References

[1] C. Appino, G. Bertotti, O. Bottauscio, F. Fiorillo, P. Tiberto, D. Binesti, J. P. Ducreux, M. Chiampi, M. Repetto, J. Appl. Phys. 79 (1996) 4575.
[2] L.R. Dupre, O. Bottauscio, M. Chiampi, M. Repetto, J.A.A. Melkebeek, IEEE Trans. Magn. 35 (1999) 4171.
[3] S.E. Zirka, Y.I. Moroz, P. Marketos, A.J. Moses, IEEE Trans. Magn. 42 (2006) 2121, http://dx.doi.org/10.1109/TMAG.2006.880685.
[4] N.P. Goss, U.S. Patent 1,965,559, 1934.
[5] F. Brailsford, R. Fogg, Proc. IEE 111 (8) (1966) 1463.
[6] J.W. Shilling, G.L. Houze, IEEE Trans. Magn. 10 (1974) 195.
[7] G. Bertotti, IEEE Trans. Magn. 24 (1988) 621.
[8] A.J. Moses, Scr. Mater. 67 (2012) 560.
[9] G. Bertotti, Hysteresis in Magnetism, Academic Press, San Diego, 1998.
[10] A. Broddefalk, M. Lindenmo, J. Magn. Magn. Mater. 304 (2006) e586, http://dx.doi.org/10.1016/j.jmmm.2006.02.183.
[11] K. Chwastek, Przegl. Elektr 5a (2012) 5.
[12] J.E.L. Bishop, J. Magn. Magn. Mater. 49 (1985) 241.
[13] B.D. Cullity, C.D. Graham, Introduction to Magnetic Materials, second ed., Wiley-IEEE Press, New York, 2009.
[14] S. Chikazumi, Physics of Ferromagnetism, second ed., Oxford University Press, Clarendon, 1997.
[15] E. Dlala, IEEE Trans. Magn. 45 (2009) 716, http://dx.doi.org/10.1109/TMAG.2008.2009878.
[16] J.R. Brauer, Z.J. Cendes, B.C. Beihoff, K.P. Phillips, IEEE Trans. Ind. Appl. 36 (2000) 1132.
[17] D. Lin, P. Zhou, W.N. Fu, Z. Badics, Z.J. Cendes, IEEE Trans. Magn. 40 (2004) 1318, http://dx.doi.org/10.1109/TMAG.2004.825025.
[18] D. Ribbenfjard, Electromagnetic Transformer Modelling Including the ferromagnetic Core (Doctoral thesis in Electrical Systems), KTH Royal Institute of Technology, Stockholm, Sweden, 2010.
[19] A. Boglietti, A. Cavagnino, M. Lazzari, M. Pastorelli, IEEE Trans. Magn. 39 (2003) 981, http://dx.doi.org/10.1109/TMAG.2003.808599.
[20] A. Lapthorn, P. Bodger, W. Enright, IEEE Trans. Power Deliv. 28 (2013) 245, http://dx.doi.org/10.1109/TPWRD.2012.2226478.
[21] H. Hamzehbahmani, P. Anderson, J. Hall, D. Fox, IEEE Trans. Power Deliv. 29 (2014) 642, http://dx.doi.org/10.1109/TPWRD.2013.2272663.
[22] S.E. Zirka, Y.I. Moroz, P. Marketos, A.J. Moses, IEEE Trans. Magn. 46 (2010) 286, http://dx.doi.org/10.1109/TMAG.2009.2032858.
[23] R.M. Bozorth, Ferromagnetism, D. Van Nostrand Company, Inc., Princeton, New Jersey, 1951.
[24] J. Avila-Rosales, F.L. Alvarado, IEEE Trans. Power Appl. Syst. 101 (1982) 4281, http://dx.doi.org/10.1109/tpas.1982.317392.
[25] J.A. Martinez, B.A. Mork, IEEE Trans. Power Deliv. 20 (2005) 1625, http://dx.doi.org/10.1109/TPWRD.2004.833884.
[26] F. de León, P. Gómez, J.A. Martinez-Velasco, M. Rioual, Transformers, in: J. A. Martinez-Velasco (Ed.), Power System Transients: Parameter Determination, CRC, Boca Raton, FL, 2009, pp. 177–249 , chapter 4.
[27] Y. Zhang, M.C. Cheng, P. Pillay, B. Helenbrook, J. Appl. Phys. 106 (2009) 043911, http://dx.doi.org/10.1063/1.3176492.
[28] S.E. Zirka, Y.I. Moroz, P. Marketos, A.J. Moses, D.C. Jiles, T. Matsuo, IEEE Trans. Magn. 44 (2008) 2113, http://dx.doi.org/10.1109/TMAG.2008.2000662.
[29] S. Zurek, P. Marketos, T. Meydan, A.J. Moses, IEEE Trans. Magn. 41 (2005) 4242, http://dx.doi.org/10.1109/TMAG.2005.854438.
[30] S.E. Zirka, Y.I. Moroz, R.G. Harrison, N. Chiesa, IEEE Trans. Power Deliv. 29 (2014) 552, http://dx.doi.org/10.1109/TPWRD.2013.2274530.
[31] S.E. Zirka, Y.I. Moroz, P. Marketos, A.J. Moses, D.C. Jiles, IEEE Trans. Magn. 42 (2006) 3177, http://dx.doi.org/10.1109/TMAG.2006.880090.
[32] W.A. Pluta, Przegląd Elektrotechniczny (Electrical Review), (2011) 37.
[33] A. Boglietti, P. Fenaris, M. Lazzari, M. Pastorelli, IEEE Trans. Magn. 31 (1995) 4250.
[34] I.D. Mayergoyz, C. Serpico, IEEE Trans. Magn. 36 (2000) 1962.
[35] C. Serpico, C. Visone, I.D. Mayergoyz, V. Basso, G. Miano, J. Appl. Phys. 87 (9) (2000) 6923 , S0021-8979~00!24808-1.
[36] I. Mayergoyz, C. Serpico, P. McAvoy, J. Appl. Phys. 109 (2011) 07E703, http://dx.doi.org/10.1063/1.3535423.
[37] W. Wolman, H. Kaden, Z. Tech. Phys. 13 (1932) 330.
[38] E.T. Stephenson, J. Appl. Phys. 57 (1) (1985) 4226.
[39] D.L. Rodrigues, J.R.F. Silveira, G.J.L. Gerhardt, F.P. Missell, F.J.G. Landgraf, R. Machado, M.F. de Campos, IEEE Trans. Magn. 48 (2012) 1425, http://dx.doi.org/10.1109/TMAG.2011.2174214.
[40] A.A. Almeida, L.S. Perassa, D.L. Rodrigues, T.S.P. Nishikawa, F.J.G. Landgraf, S. C. Paolinelli, R.V. Martins, IEEE Trans. Magn. 50 (2014) 6300404, http://dx.doi.org/10.1109/TMAG.2013.2291836.
[41] R.H. Pry, C.P. Bean, J. Appl. Phys. 29 (1958) 532, http://dx.doi.org/10.1063/1.1723212.
[42] K. Foster, F.E. Werner, R.M. Del Vecchio, J. Appl. Phys. 53 (11) (1982) 8308.
[43] Grain-Oriented, Electrical Sheet Steel Catalogue, Nippon Steel Corp., Japan, 1972.
[44] S.E. Zirka, Y.I. Moroz, A.J. Moses, C.M. Arturi, IEEE Trans. Power Deliv. 26 (2011) 2352, http://dx.doi.org/10.1109/TPWRD.2011.2140404.
[45] H.J. Williams, W. Shockley, C. Kittel, Phys. Rev. 80 (1950) 1090.
[46] F. Fiorillo, J. Magn. Magn. Mater. 242–245 (2002) 77.
[47] J.E.L. Bishop, J. Phys. D 9 (1976) 1367.
[48] S.E. Zirka, Y.I. Moroz, P. Marketos, A.J. Moses, D.C. Jiles, IEEE Trans. Magn. 44 (2008) 3189, http://dx.doi.org/10.1109/TMAG.2008.2002785.
[49] F. Colaiori, G. Durin, S. Zapperi, Phys. Rev. Lett. 97 (2006) 257203, http://dx.doi.org/10.1103/PhysRevLett.97.257203.
[50] M. Takezawa, J. Yamasaki, T. Honda, C. Kaido, J. Magn. Magn. Mater. 254–255 (2003) 167.